PAPER

CrossMark
click for updates

Understanding why replacing I₃⁻/I⁻ by cobalt(II)/(III) electrolytes in bis(diimine)copper(I)-based dye-sensitized solar cells improves performance†

Sebastian O. Fürer, Biljana Bozic-Weber, Thomas Schefer, Cedric Wobill, Edwin C. Constable, Catherine E. Housecroft* and Markus Willgert

The performances of dye-sensitized solar cells (DSCs) comprising heteroleptic bis(diimine)copper(I) based dyes combined with either $[Co(bpy)_3]^{2+/3+}$, $[Co(phen)_3]^{2+/3+}$ or I_3^-/I^- redox mediators (bpy = 2,2′-bipyridine, phen = 1,10-phenanthroline) have been evaluated. The copper(I) dyes contain the anchoring ligand ((6,6′-dimethyl-[2,2′-bipyridine]-4,4′-diyl)bis(4,1-phenylene))bis(phosphonic acid), **1**, and an ancillary ligand (**2**, **3** or **4**) with a 2,9-dimethyl-1,10-phenanthroline metal-binding domain. Ligands **2** and **3** include imidazole 2′-functionalities with 4-(diphenylamino)phenyl (**2**) or 4-(bis(4-*n*-butoxy) phenylamino)phenyl (**3**) domains; in **4**, the phen unit is substituted in the 4,7-positions with hole-transporting 4-(diphenylamino)phenyl groups. The photoconversion efficiency, η, of each of $[Cu(\mathbf{1})(\mathbf{2})]^+$, $[Cu(\mathbf{1})(\mathbf{3})]^+$ and $[Cu(\mathbf{1})(\mathbf{4})]^+$ considerably improves by replacing the I_3^-/I^- electrolyte by $[Co(bpy)_3]^{2+/3+}$ or $[Co(phen)_3]^{2+/3+}$, and after a change of electrolyte solvent (MeCN to 3-methoxypropionitrile). Due to the faster charge transfer kinetics and more positive redox potential, the cobalt-based electrolytes are superior to the I_3^-/I^- electrolyte in terms of open-circuit voltage (V_{OC}), short-circuit current (J_{SC}) and η; values of V_{OC} = 594 mV, J_{SC} = 9.58 mA cm^{-2} and η = 3.69% (relative to η = 7.12% for N719) are achieved for the best performing DSC which contains $[Cu(\mathbf{1})(\mathbf{4})]^+$ and $[Co(bpy)_3]^{2+/3+}$. Corresponding values for $[Cu(\mathbf{1})(\mathbf{4})]^+$ and I_3^-/I^- DSCs are 570–580 mV, 5.98–6.37 mA cm^{-2} and 2.43–2.62%. Electrochemical impedance spectroscopy (EIS) has been used to study DSCs with $[Cu(\mathbf{1})(\mathbf{4})]^+$ and the three electrolytes. EIS shows that the DSC with I_3^-/I^- has the highest recombination resistance, whereas the $[Co(phen)_3]^{2+/3+}$ electrolyte gives the highest chemical capacitance and V_{OC} and, between $[Co(bpy)_3]^{2+/3+}$ and $[Co(phen)_3]^{2+/3+}$, the higher recombination resistance. The $[Co(phen)_3]^{2+/3+}$ electrolyte exhibits the highest mass transport restrictions which result in a lower J_{SC} and DSC efficiency compared to the $[Co(bpy)_3]^{2+/3+}$ electrolyte.

Introduction

The Grätzel dye-sensitized solar cell (DSC)[1,2] converts solar energy into electrical power. Originally designed with ruthenium(II)-containing photosensitizers, state-of-the-art DSCs which achieve photoconversion efficiencies of ∼11–14% also use organic or zinc(II) porphyrin-based dyes.[3–15] While the sun provides an environmentally acceptable source of energy, and the concept of DSCs for energy conversion is laudable, a vision of a sustainable future demands that the components of DSCs should also originate from maintainable sources. In 1994, Sauvage and coworkers[16] demonstrated the possibility of combining bis(diimine)copper(I) dyes ($[Cu(N^\wedge N)_2]^+$) with wide band-gap n-type semiconductors (TiO₂ or ZnO) for photoconversion. While the photophysical properties of $[Cu(N^\wedge N)_2]^+$ complexes continued to be a focus of attention,[17,18] no real progress in applying this family of complexes as sensitizers in DSCs was made until Sakaki in 2002 [19] and our own reports in 2008.[20] Since then, there have been significant advances in the design both of ligands to anchor $[Cu(N^\wedge N)_2]^+$ sensitizers to an FTO/TiO₂ surface and promote electron injection from dye to semiconductor, and of ancillary ligands to improve light absorption and optimize electron transfer between electrolyte and dye.[21,22] To date, the best photoconversion efficiencies, η, in copper-based DSCs have been achieved using heteroleptic dyes. Efficiencies passed 3% (fully masked DSCs[23,24]) in 2014,[25] and the current record is 4.66% reported by Odobel and coworkers;[26] both values are with respect to η ∼ 7.5% for the reference dye N719. Heteroleptic dyes have the advantage over homoleptic dyes in being able to combine optimally designed anchoring and ancillary domains.

Department of Chemistry, University of Basel, Spitalstrasse 51, CH-4056 Basel, Switzerland. E-mail: catherine.housecroft@unibas.ch

This journal is © The Royal Society of Chemistry 2016

J. Mater. Chem. A, 2016, 4, 12995–13004 | 12995

While ligand design is of crucial importance, appropriate combinations of dye and electrolyte are also key to optimizing DSC performance. The maximum voltage generated under illumination (the open-circuit voltage, V_{OC}) is the difference between the redox potential of the electrolyte and the Fermi level of the TiO_2 semiconductor. The I_3^-/I^- redox shuttle is ubiquitous among liquid electrolytes in DSCs and is used in many studies of copper-based DSCs.[21] However, the I_3^-/I^- electrolyte composition has been optimized for ruthenium(II)-based cells.[27,28] A way to enhance the photoconversion efficiencies of DSCs containing copper-dyes is to increase V_{OC}, and this can, in principle, be achieved by employing an electrolyte with a redox potential that is more positive than that of I_3^-/I^-. Among the range of iodine-free redox mediators that have been investigated,[29,30] those based on the Co^{3+}/Co^{2+} redox couple[31,32] are superior. The use of a $[Co(phen)_3]^{3+/2+}$ (phen = 1,10-phenanthroline) electrolyte contributed to the current record DSC photoconversion efficiency of 14.3%.[15] The redox potentials of $[Co(phen)_3]^{3+/2+}$ and $[Co(bpy)_3]^{3+/2+}$ (bpy = 2,2'-bipyridine) are +0.61 V and +0.56 V, respectively,[29] compared to +0.35 V for I_3^-/I^- (in MeCN and vs. NHE);[28,29] values are solvent dependent and values of +0.72, +0.65 and +0.31 V (vs. NHE), respectively, are also tabulated.[32] Drawbacks of cobalt-based electrolytes are the larger size of the $[Co(diimine)_3]^{n+}$ ions which leads to mass transport problems, less efficient charge transfer at the Pt counter electrode compared to that with an I_3^-/I^- redox shuttle, and fast recombination of electrons between the photoanode and the oxidized (Co^{3+}) redox couple.[33,34]

While the use of cobalt-based electrolytes with ruthenium-containing and organic dyes is well established, combining the Co^{3+}/Co^{2+} redox couple with copper-based sensitizers has been little explored. Both we[35] and Ashbrook and Elliott[36] have demonstrated the compatibility of bis(diimine)copper(I) dyes with $[Co(4,4'-R_2bpy)_3]^{3+/2+}$ (R = H[35] or ^tBu[36]) redox mediators, but no investigations have addressed the optimization of the electrolyte composition. We now report the results of a study of the performances of DSCs containing three heteroleptic $[Cu(L_{anchor})(L_{ancillary})]^+$ sensitizers in the presence of $[Co(bpy)_3]^{3+/2+}$ or $[Co(phen)_3]^{3+/2+}$ electrolytes of varying compositions and reinforce the fact that $Co^{3+/2+}$ redox mediators are compatible with copper(I)-based DSCs. We also demonstrate the benefits of changing the solvent in the electrolyte from MeCN to the less volatile 3-methoxypropionitrile. Electrochemical impedance spectroscopy is used to understand the differences between the iodine and cobalt-based electrolytes in bis(diimine)copper(I)-based DSCs.

Experimental

Materials

Ligand 1[37] and the homoleptic complexes $[Cu(2)_2][PF_6]$, $[Cu(3)_2][PF_6]$ and $[Cu(4)_2][PF_6]$,[35,38] were prepared as previously described.

DSC fabrication

The FTO/Pt counter electrodes were purchased from Solaronix (Solaronix Test Cell kit). The FTO/TiO_2 electrodes were prepared in-house by screen printing as previously described;[35] the annealed TiO_2 film was post-treated with 60 mM aqueous $TiCl_4$ solution.[35] Each working electrode was heated to 500 °C and allowed to cool to 80 °C prior to dipping into a 1 mM solution of the anchoring ligand 1 (Scheme 1) for 1 day. The electrodes were washed with DMSO and EtOH, and then dried in a stream of N_2. The electrodes were soaked in a 0.1 mM MeCN solution of $[Cu(L_{ancillary})_2][PF_6]$ ($L_{ancillary}$ = 2, 3 or 4, Scheme 1) for 3 days after which it was washed with MeCN and dried in N_2. The DSCs were assembled by combining the working electrode and counter electrode (Solaronix Test Cell Platinum Electrode, heated on a heating plate at 450 °C for 30 min to remove volatile organic impurities) by using a thermoplast hot-melt sealing foil (Solaronix, Meltonix 1170-60), then filled with the respective electrolyte by vacuum-backfilling. The DSC was closed using thermoplast hot-melt sealing foil and a cover glass. N719 reference electrodes were made by immersing screen-printed[35] FTO/TiO_2 electrodes (post-treated with 40 mmol dm^{-3} aqueous $TiCl_4$) in a 0.3 mM EtOH solution of N719 (Solaronix) for 3 days. The electrodes were removed from the dye-bath, washed with EtOH, and dried in a stream of N_2.
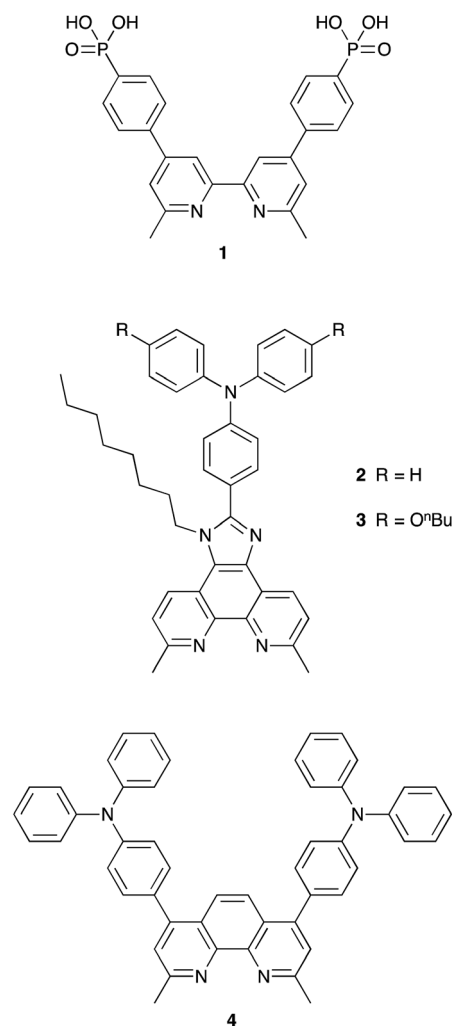
Scheme 1 Structures of anchoring ligand 1 and ancillary ligands 2–4.

The I_3^-/I^- electrolyte comprised LiI (0.1 M), I_2 (0.05 M), 1-methylbenzimidazole (0.5 M), 1-butyl-3-methylimidazolinium iodide (0.6 M) in 3-methoxypropionitrile. $[Co(bpy)_3][PF_6]_2$ and $[Co(phen)_3][PF_6]_2$ were prepared from $CoCl_2 \cdot 6H_2O$ as described in the literature.[39] $[Co(bpy)_3][PF_6]_3$ and $[Co(phen)_3][PF_6]_3$ were prepared by oxidation of the corresponding cobalt(II) complex using $[NO][BF_4]$ followed by anion exchange with $[NH_4][PF_6]$; the ^1H NMR spectra matched literature data.[40] See Table 1 for electrolyte compositions.

DSC measurements

J–V measurements were performed using a SolarSim 150 (Solaronix) or LOT Quantum Design LS0811 sun simulator, which was calibrated with a Si-reference cell to 1000 W m^{-2} prior to the measurements. All cells were completely masked.[23,24] Voltage decay was measured on a ModuLab XM electrochemical system.

Electrochemical impedance spectroscopy (EIS) measurements were carried out on a ModuLab® XM PhotoEchem photoelectrochemical measurement system setup from Solartron Analytical. The impedance was measured at steady state close to the open-circuit potential of the cell at different light intensities (LED, 590 nm) in the frequency range 0.05 Hz to 400 kHz using an amplitude of 10 mV. The impedance data was fitted to an equivalent circuit model and analysed using ZView® software from Scribner Associates Inc.

Results and discussion

Choice of sensitizers

The heteroleptic copper(I) dyes chosen for the present study are three of a series of sensitizers that we have previously studied in combination with I_3^-/I^- electrolyte in DSCs.[38] All contain the phosphonic acid anchoring ligand **1** (Scheme 1); for copper(I) dyes, we have found phosphonic acids to be superior over analogous carboxylic acid anchors.[41] Phosphonic acid anchors are also used in ruthenium-based dyes,[42] and the strong surface binding is advantageous with respect to carboxylic acid anchors. However, we note that in terms of the rate of electron injection, carboxylic acid anchors may be favoured over phosphonic acids.[43] The ancillary ligands **2–4** (Scheme 1) contain a phen metal-binding unit and one or two triphenylamino-domains to enhance light-absorption. Ligands **2** and **3** feature a long alkyl chain to militate against dye-molecule aggregation by intermolecular π-stacking.[44] Ligand **3** contains n-butoxy chains on the triphenylamino-unit which are known to improve

the performance of DSCs employing triphenylamine-containing organic sensitizers in combination with cobalt electrolytes.[31] Due to the steric hindrance of the n-butoxy chains, electron recombination with the electrolyte, which previously was reported to be one of the main issues with this kind of mediator,[39] is significantly reduced. All ligands contain methyl substituents adjacent to the N,N'-coordination site to stabilize the copper(I) dyes (tetrahedral, Scheme 2) against irreversible oxidation to copper(II) (square planar).

The copper(I) dyes were assembled *in situ* on FTO/TiO$_2$ electrodes using a 'surfaces-as-ligands' approach which we have established as being effective for complexes which are labile in solution.[21] Screen-printed mesoporous TiO$_2$ electrodes with scattering layer were post-treated with aqueous TiCl$_4$ solution using conditions that we have previously optimized.[35] Each electrode was immersed in a solution of the phosphonic acid anchoring ligand **1** followed by soaking in a dye-bath containing either $[Cu(2)_2][PF_6]$, $[Cu(3)_2][PF_6]$ or $[Cu(4)_2][PF_6]$. Ligand exchange leads to the formation of the surface-anchored dyes $[Cu(1)(2)]^+$ (eqn (1)), $[Cu(1)(3)]^+$ or $[Cu(1)(4)]^+$. By eye, the orange colour of the electrodes was consistent with the presence of adsorbed dye, and this was quantified by solid-state absorption spectroscopy using electrodes assembled as described in the
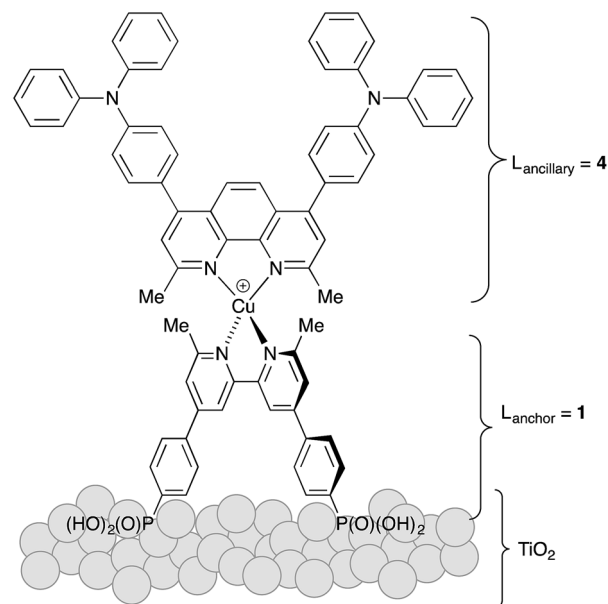
Scheme 2 Surface-adsorbed dye $[Cu(1)(4)]^+$ as an example of the three sensitizers investigated.

Table 1 Compositions of electrolytes; TBP = 4-*tert*-butylpyridine, MPN = 3-methoxypropionitrile

Component	Electrolyte E1	Electrolyte E2	Electrolyte E3	Electrolyte E4
Co^{2+}	$[Co(bpy)_3][PF_6]_2$ (0.2 M)	$[Co(phen)_3][PF_6]_2$ (0.2 M)	$[Co(bpy)_3][PF_6]_2$ (0.2 M)	$[Co(phen)_3][PF_6]_2$ (0.175 M)
Co^{3+}	$[Co(bpy)_3][PF_6]_3$ (0.05 M)	$[Co(phen)_3][PF_6]_3$ (0.05 M)	$[Co(bpy)_3][PF_6]_3$ (0.05 M)	$[Co(phen)_3][PF_6]_3$ (0.044 M)
LiClO$_4$	0.1 M	0.1 M	0.1 M	0.088 M
TBP	0.2 M	0.2 M	0.2 M	0.175 M
Solvent	MeCN	MeCN	MPN	MPN

This journal is © The Royal Society of Chemistry 2016

J. Mater. Chem. A, 2016, 4, 12995–13004 | 12997

Experimental section but without the scattering layer. The observed absorption maxima ($\lambda_{max} \sim 470$ nm) were consistent with those already reported.[38]

$$FTO/TiO_2/\mathbf{1} + [Cu(\mathbf{2})_2]^+ \rightarrow FTO/TiO_2/[(\mathbf{1})Cu(\mathbf{2})]^+ + \mathbf{2} \quad (1)$$

Co^{2+}/Co^{3+} electrolytes in acetonitrile

The compositions of the Co^{2+}/Co^{3+} electrolytes are given in Table 1. Initially, we used MeCN as the solvent and the compositions of electrolytes E1 and E2 are typical of Co^{2+}/Co^{3+} electrolytes employing bpy or phen ligands. The first sensitizer to be investigated was $[Cu(\mathbf{1})(\mathbf{3})]^+$. The open-circuit voltage (V_{OC}), short-circuit current density (J_{SC}), fill factor (ff) and photoconversion efficiency (η) were measured immediately after sealing the DSCs; cells were masked, and reproducibility of the data was checked by using duplicate cells (Table 2). Table 2 also gives performance characteristics of a reference DSC containing the standard ruthenium dye N719 combined with an I_3^-/I^- electrolyte. The right-hand column in Table 2 gives a relative η, setting the value for an N719 reference DSC to 100%. We routinely use two sun simulators (LOT Quantum Design LS0811 and SolarSim 150 instruments) and, as previously discussed,[45] DSC characteristics for the same cell recorded on the same day on these instruments (both under irradiation of 1 sun) lead to similar values of V_{OC} but different values of J_{SC}. By using relative η values, we can justifiably compare data measured on different instruments.[45]

Table 2 shows that there is an increase in both J_{SC} and V_{OC} on changing from $[Co(bpy)_3]^{2+/3+}$ to $[Co(phen)_3]^{2+/3+}$ (from electrolyte E1 to E2). The relative efficiencies of 33.8 and 38.1% for the $[Co(bpy)_3]^{2+/3+}$-containing DSCs, and 42.5 and 45.0% for the $[Co(phen)_3]^{2+/3+}$-containing DSCs are appreciably higher than the 22.5 and 25.7% observed for $[Cu(\mathbf{1})(\mathbf{3})]^+$ combined with a standard I_3^-/I^- electrolyte (Table S1†).[38] Although the data were extremely promising, we experienced difficulties with the use of MeCN as solvent. Firstly, the DSCs tended to be unstable, performing poorly after several days. When the dye $[Cu(\mathbf{1})(\mathbf{4})]^+$ was combined with electrolyte E1, orange crystals rapidly formed in the sealed DSC (Fig. 1). Rapid crystal growth was a persistent problem in DSCs containing a combination of $[Cu(\mathbf{1})(\mathbf{4})]^+$ and $[Co(bpy)_3]^{2+/3+}$. Attempts to analyse the crystals by mass spectrometry and X-ray crystallography did not provide definitive identification of the crystalline material. Crystals were
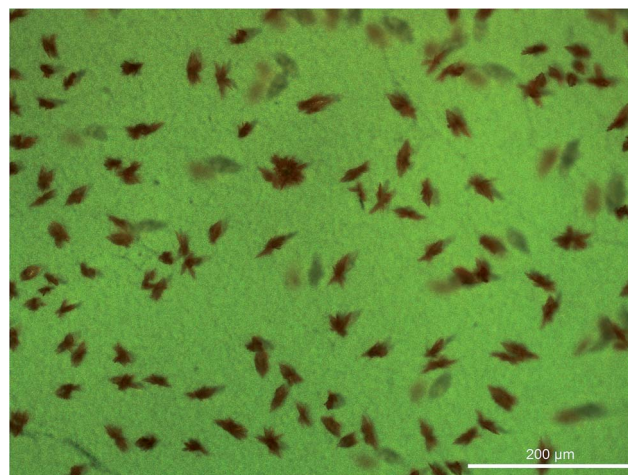

Fig. 1 Crystal formation in sealed DSCs containing electrolyte E1 and the dye $[Cu(\mathbf{1})(\mathbf{4})]^+$ (Leica MC170 HD microscope).

also observed in DSCs containing $[Cu(\mathbf{1})(\mathbf{4})]^+$ and $[Co(phen)_3]^{2+/3+}$, although their growth was slower than in electrolyte E1; a substantial fall in J_{SC} was observed after two or more days. The formation of crystals of $(MBI)_6(HMBI^+)_2(I^-)(I_3^-)$ (MBI = N-methylbenzimidazole) from electrolyte components in DSCs has previously been reported,[46] but of course, this salt cannot be responsible for the crystals observed in the cobalt-based electrolytes. Other than this latter report, precipitation or crystal formation from liquid electrolytes in DSCs does not appear to have been discussed in detail in the literature.[47]

Co^{2+}/Co^{3+} electrolytes in 3-methoxypropionitrile

The problems encountered with the combination of $[Cu(\mathbf{1})(\mathbf{4})]^+$ and electrolytes E1 or E2 led us to change the solvent to 3-methoxypropionitrile (MPN) which is widely employed in DSCs.[6,47] Electrolyte E3 differs from E1 only in the solvent variation (Table 1). However, the lower solubility of $[Co(phen)_3][PF_6]_3$ in MPN compared to MeCN resulted in the use of a 0.044 M solution of $[Co(phen)_3][PF_6]_3$ in electrolyte E4 rather than the preferred 0.05 M. The concentrations of the other electrolyte components were reduced to maintain the same molar ratios in E3 and E4 (Table 1). Table 3 gives the performance parameters of masked, duplicate cells for each dye/electrolyte combination, and

Table 2 Performance parameters[a] on the day of sealing the DSCs for duplicate cells (numbered 1 and 2) combining dye $[Cu(\mathbf{1})(\mathbf{3})]^+$ with electrolytes E1 or E2 (MeCN solvent, see Table 1). A reference N719 DSC was also measured

Dye	Electrolyte	Cell number	J_{SC}/mA cm^{-2}	V_{OC}/mV	ff/%	η/%	Relative[b] η/%
$[Cu(\mathbf{1})(\mathbf{3})]^+$	E1 (bpy)	1	5.30	640	69	2.32	38.1
$[Cu(\mathbf{1})(\mathbf{3})]^+$	E1 (bpy)	2	5.45	652	58	2.06	33.8
$[Cu(\mathbf{1})(\mathbf{3})]^+$	E2 (phen)	1	5.91	735	63	2.74	45.0
$[Cu(\mathbf{1})(\mathbf{3})]^+$	E2 (phen)	2	5.88	731	60	2.59	42.5
N719[b]	I_3^-/I^-		13.8	705	63	6.09	100

[a] Measurements were made on a LOT Quantum Design LS0811 sun simulator. [b] Relative η is relative to N719 set at 100%.

Table 3 Performance parameters[a] on the day of sealing the DSCs for duplicate cells (numbered 1 and 2) combining dyes [Cu(**1**)(**2**)]$^+$, [Cu(**1**)(**3**)]$^+$ or [Cu(**1**)(**4**)]$^+$ with electrolytes E3 or E4 (MPN solvent). A reference N719 DSC was also measured

| Dye	Electrolyte	Cell number	J_{SC}/mA cm^{-2}	V_{OC}/mV	ff/%	η/%	Relative[b] η/%
[Cu(**1**)(**2**)]$^+$	E3 (bpy)	1	6.98	596	66	2.75	38.6
[Cu(**1**)(**2**)]$^+$	E3	2	6.41	605	62	2.41	33.8
[Cu(**1**)(**3**)]$^+$	E3	1	8.24	583	61	2.92	41.0
[Cu(**1**)(**3**)]$^+$	E3	2	8.66	619	65	3.50	49.2
[Cu(**1**)(**4**)]$^+$	E3	1	9.06	598	64	3.47	48.7
[Cu(**1**)(**4**)]$^+$	E3	2	9.58	594	65	3.69	51.8
[Cu(**1**)(**2**)]$^+$	E4 (phen)	1	7.68	559	64	2.73	38.3
[Cu(**1**)(**2**)]$^+$	E4	2	7.15	530	64	2.42	34.0
[Cu(**1**)(**3**)]$^+$	E4	1	8.61	637	61	3.34	46.9
[Cu(**1**)(**3**)]$^+$	E4	2	8.14	643	56	2.92	41.0
[Cu(**1**)(**4**)]$^+$	E4	1	8.54	620	60	3.17	44.5
[Cu(**1**)(**4**)]$^+$	E4	2	8.57	622	60	3.17	44.5
N719[b]	I$_3^-$/I$^-$		17.13	650	64	7.12	100

[a] Measurements were made on a SolarSim 150 sun simulator. [b] Relative η is relative to N719 set at 100%.

the corresponding *J–V* curves for the better performing DSC from each pair are depicted in Fig. 2.

Irrespective of the cobalt complex used in the electrolyte, DSCs containing sensitizers [Cu(**1**)(**3**)]$^+$ or [Cu(**1**)(**4**)]$^+$ exhibit higher values of J_{SC} and V_{OC} than those containing [Cu(**1**)(**2**)]$^+$. The superior performance of [Cu(**1**)(**4**)]$^+$ is consistent with the results obtained using an I$_3^-$/I$^-$ electrolyte[38] (Table S1†). Most importantly, the observed values of J_{SC} for DSCs with cobalt electrolytes are substantially higher than for the same dyes with an I$_3^-$/I$^-$ electrolyte; values of J_{SC} = 9.58 and 9.06 mA cm^{-2} for [Cu(**1**)(**4**)]$^+$ with electrolyte E3 (Table 3) compare with a range of 5.98–6.81 mA cm^{-2} for [Cu(**1**)(**4**)]$^+$ with I$_3^-$/I$^-$ (Tables S1 and S2†). For the dyes [Cu(**1**)(**3**)]$^+$ and [Cu(**1**)(**4**)]$^+$, higher values of V_{OC} are observed for electrolyte E4 than for E3, consistent with the more positive redox potential of the [Co(phen)$_3$]$^{2+/3+}$ couple *versus* [Co(bpy)$_3$]$^{2+/3+}$.[29,32] On the other hand, higher values of J_{SC} are obtained for both [Cu(**1**)(**3**)]$^+$ and [Cu(**1**)(**4**)]$^+$ when the redox mediator is [Co(bpy)$_3$]$^{2+/3+}$. In terms of DSC efficiencies (Table 3), the use of [Co(bpy)$_3$]$^{2+/3+}$ is superior to [Co(phen)$_3$]$^{2+/3+}$.

Fig. 3 shows the EQE spectra of DSCs containing the dyes combined with the [Co(bpy)$_3$]$^{2+/3+}$ redox shuttle. The first point to note is the differences in the shapes of the EQE spectra compared to the corresponding spectra for the same dyes in combination with I$_3^-$/I$^-$ electrolyte (Fig. S1†). The gain in EQE in the region between 370 and 420 nm reflects the competing light absorption[34,48] of I$_3^-$ which reduces the number of photons being harvested by the copper dyes. Values of EQE$_{max}$ show a marked increase on going from an I$_3^-$/I$^-$ to [Co(bpy)$_3$]$^{2+/3+}$ redox mediator (Table 4). A comparison of Fig. 3 and S1† also reveals enhanced quantum efficiency at higher wavelengths (570–620 nm) for all three dyes.

The mass transport problem that is known to affect [Co(diimine)$_3$]$^{n+/(n-1)+}$ redox mediators[47] can be investigated by measuring the dependence of J_{SC} for a given DSC on the incident light intensity.[34] The DSC parameters for duplicate cells containing [Cu(**1**)(**3**)]$^+$ or [Cu(**1**)(**4**)]$^+$ and electrolyte E4 measured under different light intensities are given in Table 5. In keeping with the use of the I$_3^-$/I$^-$ electrolyte in the N719 reference DSC,
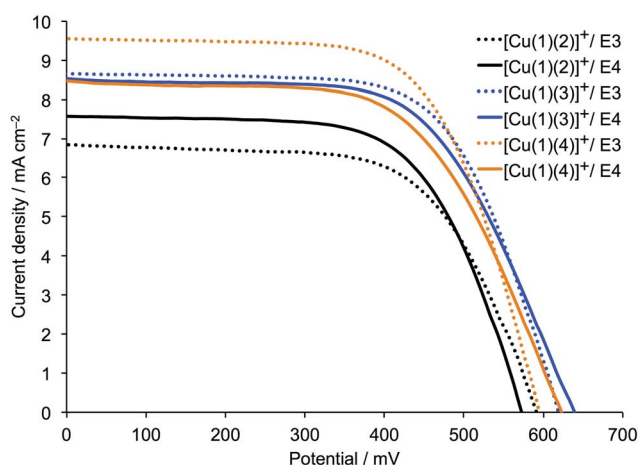
Fig. 2 *J–V* curves measured on the day of sealing DSCs containing the dyes [Cu(**1**)(**2**)]$^+$, [Cu(**1**)(**3**)]$^+$ or [Cu(**1**)(**4**)]$^+$ and electrolytes E3 or E4 (see Table 1).
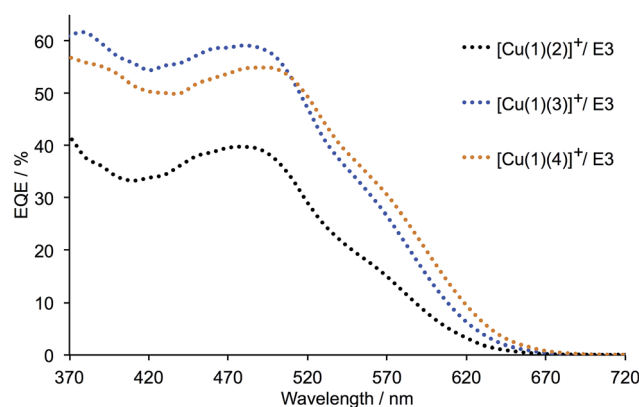
Fig. 3 EQE spectra of DSCs containing the dyes [Cu(**1**)(**2**)]$^+$, [Cu(**1**)(**3**)]$^+$ or [Cu(**1**)(**4**)]$^+$ and electrolyte E3 (with [Co(bpy)$_3$]$^{2+/3+}$). The spectrum for the better performing DSC of each pair measured for each dye is shown; see also Table 3.

This journal is © The Royal Society of Chemistry 2016

J. Mater. Chem. A, 2016, **4**, 12995–13004 | **12999**

Table 4 EQE maxima for duplicate DSCs containing the sensitizers $[Cu(1)(2)]^+$, $[Cu(1)(3)]^+$ and $[Cu(1)(4)]^+$ combined with electrolyte E3 (with $[Co(bpy)_3]^{2+/3+}$) or I_3^-/I^-

Dye	Electrolyte	EQE$_{max}$/%	λ/nm	
$[Cu(1)(2)]^+$	E3	39.8 (sh. 17.4)	480 (sh. 560)	This work
$[Cu(1)(2)]^+$	E3	37.0 (sh. 15.7)	480 (sh. 560)	This work
$[Cu(1)(2)]^+$	I_3^-/I^-	37.9	480	Ref. 38
$[Cu(1)(2)]^+$	I_3^-/I^-	35.3	480	Ref. 38
$[Cu(1)(3)]^+$	E3	59.1 (sh. 30.4)	480 (sh. 550)	This work
$[Cu(1)(3)]^+$	E3	56.1 (sh. 30.0)	480 (sh. 550)	This work
$[Cu(1)(3)]^+$	I_3^-/I^-	37.3	480	Ref. 38
$[Cu(1)(3)]^+$	I_3^-/I^-	34.7	480	Ref. 38
$[Cu(1)(4)]^+$	E3	54.9 (sh. 30.6)	490 (sh. 570)	This work
$[Cu(1)(4)]^+$	E3	51.3 (sh. 29.3)	490 (sh. 570)	This work
$[Cu(1)(4)]^+$	I_3^-/I^-	36.6 (sh. 19.5)	490 (sh. 570)	Ref. 38
$[Cu(1)(4)]^+$	I_3^-/I^-	37.1 (sh. 19.5)	490 (sh. 570)	Ref. 38

there is an approximately linear dependence of J_{SC} on light intensity and the photoconversion efficiency is essentially constant. However, the mass transport problem associated with $[Co(phen)_3]^{2+/3+}$ (electrolyte E4) manifests itself in the non-linear dependence between J_{SC} and light intensity seen in Table 5 for each DSC containing the dyes $[Cu(1)(3)]^+$ or $[Cu(1)(4)]^+$.

Overall, we observe a marked improvement in the photo-conversion efficiencies of all three sensitizers in DSCs on going from an I_3^-/I^- to a $[Co(bpy)_3]^{2+/3+}$ or $[Co(phen)_3]^{2+/3+}$ electrolyte using MPN as solvent. The most promising combination of an FTO/TiO$_2$/$[Cu(1)(4)]^+$ photoanode in conjunction with a $[Co(bpy)_3]^{2+/3+}$ redox mediator where efficiencies of 3.47 and 3.69% were achieved; relative to the N719 reference DSC, these values correspond to relative η values of 48.7 and 51.8%. Significantly, the values of $\eta = 3.47$ and 3.69% are the highest efficiencies achieved for a heteroleptic copper(I) sensitizer using the 'surfaces-as-ligands' approach, the previous record being 3.16% with respect to 7.63% for N719.[25]

Electrochemical impedance spectroscopy (EIS)

EIS was used to evaluate the electrochemical behaviour of the DSCs in more detail. This technique allows one to measure the internal impedances of the DSC, and key parameters including the recombination resistance (R_{rec}), chemical capacitance (C_μ) and the electron lifetime (τ) (which is the product of R_{rec} and C_μ), can be obtained.[49,50] Three sets of duplicate DSCs were used in the investigation. All DSCs contained the sensitizer $[Cu(1)(4)]^+$ which was shown in the studies described above to be the best performing of $[Cu(1)(2)]^+$, $[Cu(1)(3)]^+$ and $[Cu(1)(4)]^+$. Each set of DSCs used a different redox mediator ($[Co(bpy)_3]^{2+/3+}$, $[Co(phen)_3]^{2+/3+}$ or I_3^-/I^-). The electrolyte compositions for the cobalt-based electrolytes are given in Table 1. The DSCs in the EIS study correspond to those in Table 3 with electrolytes E3 and E4, and to the DSCs from a set made using $[Cu(1)(4)]^+$ and a standard I_3^-/I^- electrolyte (Table S2†) which showed 2.43 and 2.46% efficiencies. The performances of these I_3^-/I^--containing DSCs are consistent with previously published data.[38] Measured EIS data at two different light intensities are presented in Tables 6 and 7. Table 6 shows the impedance spectra of the DSCs, with one cell of each configuration measured at a bias light intensity of 22 mW cm^{-2}. At this light intensity, the transport resistance (R_t) of the electrons in the semiconducting TiO$_2$ is negligible. Furthermore, at this light intensity, the V_{OC} values follow the same trend as those found in the J–V measurements under 1 sun (see Tables 3 and S2†), where electrolyte E4 gives the highest V_{OC} values for $[Cu(1)(4)]^+$. Table 7 shows the parameters obtained at low light intensity, where the transport resistance, R_t, can be studied. L_d which is the length of electron diffusion "backwards" in the semi-conductor should, in a well performing DSC electrode, be at least as long as the thickness of the porous TiO$_2$ layer L to minimize back reactions.[50] Hence, $L_d/L > 1$ must be fulfilled, since this implies that transit time in the semi-conductor is shorter than the electron lifetime. Pleasingly, in all DSCs measured in this study (Table 7), L_d (which is calculated as the square root of R_{rec}/R_t) is larger than L, and

Table 5 Performance parameters[a] on the day of sealing duplicate DSCs (numbered 1 and 2) combining the dyes $[Cu(1)(3)]^+$ or $[Cu(1)(4)]^+$ with electrolyte E4 (MPN solvent). A reference N719 DSC with I_3^-/I^- electrolyte was also measured

Dye	Cell number	Light intensity[b]/%	J_{SC}/mA cm^{-2}	V_{OC}/mV	ff/%	η/%
$[Cu(1)(3)]^+$	1	100	4.32	632	65	1.79
$[Cu(1)(3)]^+$	1	50	2.93	598	68	2.39
$[Cu(1)(3)]^+$	1	10	0.75	543	72	2.95
$[Cu(1)(3)]^+$	2	100	4.26	634	64	1.73
$[Cu(1)(3)]^+$	2	50	2.85	605	69	2.37
$[Cu(1)(3)]^+$	2	10	0.65	544	73	2.59
$[Cu(1)(4)]^+$	1	100	4.07	609	61	1.52
$[Cu(1)(4)]^+$	1	50	2.92	587	65	2.23
$[Cu(1)(4)]^+$	1	10	0.79	540	72	3.05
$[Cu(1)(4)]^+$	2	100	4.05	620	57	1.43
$[Cu(1)(4)]^+$	2	50	3.04	600	61	2.24
$[Cu(1)(4)]^+$	2	10	0.81	552	72	3.21
N719	1	100	11.77	690	72	5.89
N719	1	50	5.82	664	74	5.71
N719	1	10	1.32	597	73	5.74

[a] Measurements were made on a LOT Quantum Design LS0811. [b] 100% light intensity = 1 sun = 1000 W m^{-2}.

13000 | J. Mater. Chem. A, 2016, 4, 12995–13004

This journal is © The Royal Society of Chemistry 2016

Table 6 Impedance data obtained during measurements at 22 mW cm^{-2}. EIS measurements are carried out 1 day after DSC assembly. See Table 1 for E3 and E4 electrolyte compositions

Electrolyte used with dye [Cu(**1**)(**4**)]$^+$	R_d/Ω	R_{rec}/Ω	$C_\mu/\mu F$	R_{Pt}/Ω	$C_{Pt}/\mu F$	τ/ms	V_{OC}/mV	η^a/%
E3 (bpy) cell 1	112	86	479.3	7	4.5	41	646	3.47
E3 (bpy) cell 2	97	72	507.8	7	4.3	36	641	3.69
E4 (phen) cell 1	171	107	646.1	15	5.5	69	661	3.17
E4 (phen) cell 2	157	103	641.2	31	2.3	66	665	3.17
I$_3^-$/I$^-$ cell 1	5	224	461.8	8	5.6	103	579	2.73
I$_3^-$/I$^-$ cell 2	6	188	486.8	10	5.2	91	593	2.62

^{a} The cell efficiency is that of the particular cell measured with EIS.

Table 7 Impedance data obtained during measurements at 0.44 mW cm^{-2}. EIS measurements are carried out 1 day after DSC assembly. See Table 1 for E3 and E4 electrolyte compositions

Electrolyte used with dye [Cu(**1**)(**4**)]$^+$	R_t/Ω	R_{rec}/Ω	$C_\mu/\mu F$	R_{Pt}/Ω	$C_{Pt}/\mu F$	τ/ms	L_d/L (dimensionless)	V_{OC}/mV
E3 (bpy) cell 1	93	2360	125.6	5	8.5	296	5	515
E3 (bpy) cell 2	47	2079	141.0	6	4.9	293	7	515
E4 (phen) cell 1	87	2753	162.3	15	6.3	447	6	518
E4 (phen) cell 2	61	2325	180.3	29	2.3	419	6	540
I$_3^-$/I$^-$ cell 1	40	6817	172.4	8	5.5	1175	13	462
I$_3^-$/I$^-$ cell 2	35	5478	200.3	11	4.9	1097	12	474

significantly so for the I$_3^-$/I$^-$ electrolyte cells, due to their higher R_{rec} and lower transport resistance.

From Table 6, Fig. 4 and 5c, it can be seen that the diffusion resistance, R_d (which is represented as the third arc from the left in each spectrum in Fig. 4a for DSCs with cobalt-electrolytes) is considerably pronounced. This particular arc is, however, barely seen in the spectrum for the DSC containing the I$_3^-$/I$^-$ based redox mediator. The relatively bulky cobalt complexes restrict the mass transport and lower the diffusion coefficient compared to the iodide system.[34,51] Furthermore, it is clearly seen that R_d is larger for the [Co(phen)]$^{2+/3+}$ than for the [Co(bpy)$_3$]$^{2+/3+}$.

The recombination resistance, R_{rec}, is generally lower for the DSCs having cobalt electrolytes compared to I$_3^-$/I$^-$ (Table 6, Fig. 5b). This is also seen in the Nyquist plot in Fig. 4a, as the magnitude of R_{rec} (which is represented by the second arc from the left in each spectrum) is significantly larger for the DSC having the I$_3^-$/I$^-$ electrolyte. This is in agreement with the fast electron transfer from I$^-$ to regenerate the dye compared to the lower rate of reduction of I$_3^-$ which minimizes the back reaction interfacial process (higher R_{rec}).[52] For the cobalt-based electrolytes, the consequence is that the faster back reaction kinetics of the cobalt mediators decrease R_{rec} in accordance with the discussion above. However, the simpler outer sphere electron transfer of the cobalt redox mediators (in contrast to the iodide species, which involve the creation and breaking of chemical bonds as opposed to simple electron transfer),[40] give the cobalt DSCs their higher J_{SC} and chemical capacitance, C_μ. C_μ is related to the total density of electrons in the semiconductor and typically rises exponentially at higher light intensities;[49] this is also seen in Fig. 5a. R_t, which is strongly
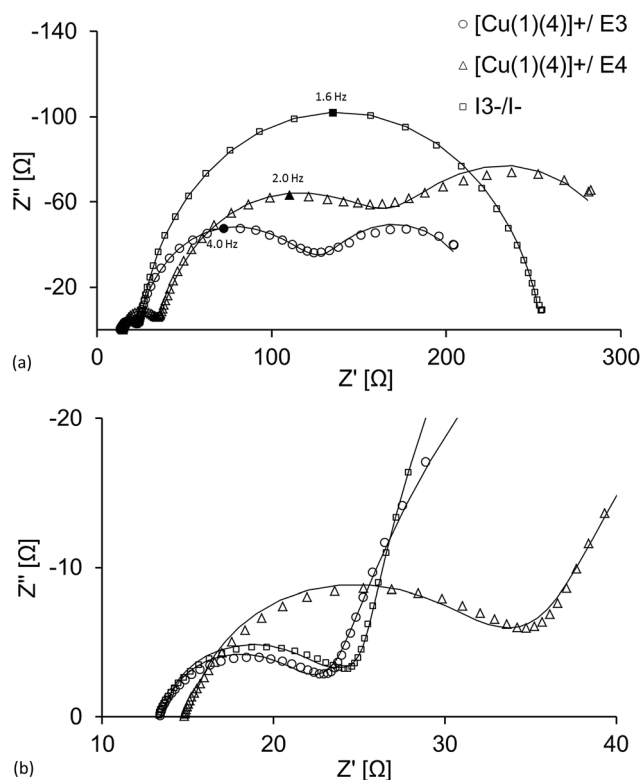
Fig. 4 (a) Nyquist plot from EIS measurements of three DSCs having the electrolyte systems E3, E4 and I$_3^-$/I$^-$, and (b) a zoom-in of the high frequency region. The larger R_{rec} of the I$_3^-$/I$^-$-based system as well as the pronounced R_d of the cobalt-based electrolytes are clearly seen. The graphs presented here are the ones from each of the duplicate cells denoted 'cell 1'.
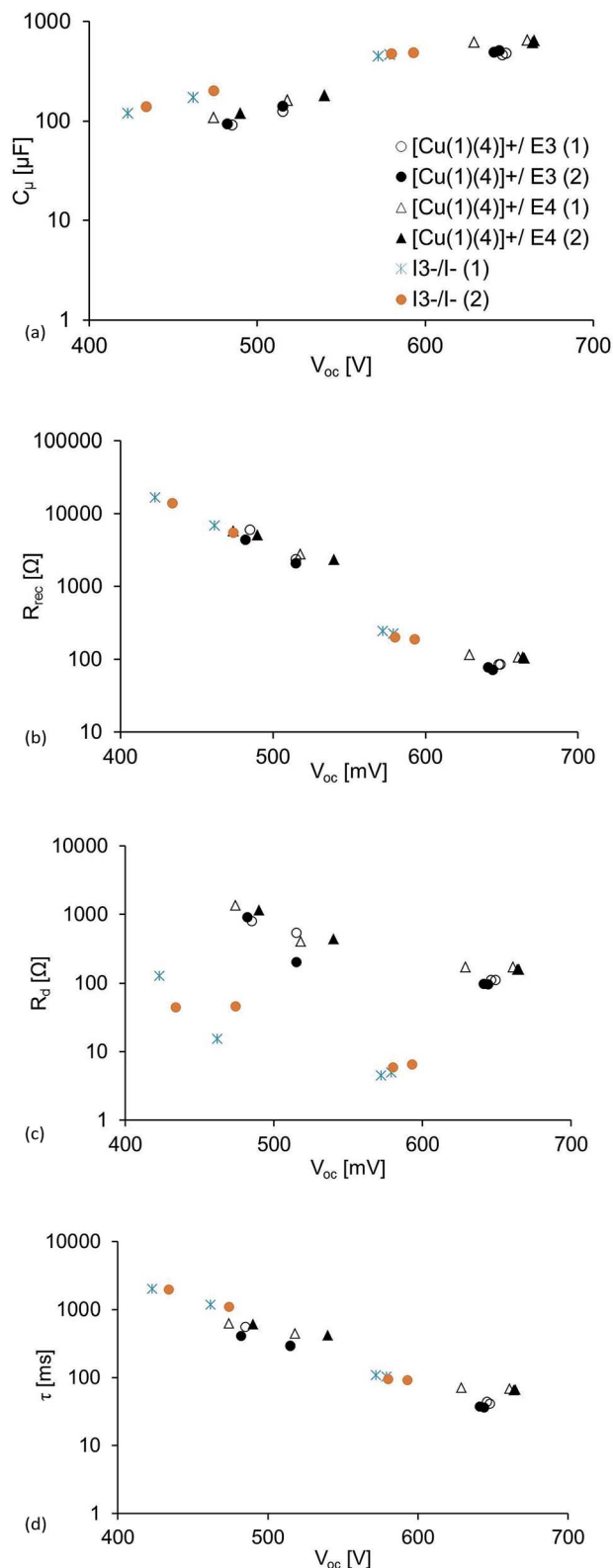
Fig. 5 Plots of the parameters at different light intensities (0.22, 0.44, 13.2 and 22.0 mW cm^{-2}) against V_{OC}: (a) chemical capacitance, (b) recombination resistance, (c) diffusion resistance and (d) electron lifetime. For light intensities of 0.44 and 22 mW cm^{-2}, values of V_{OC} are given in Tables 6 and 7. Each V_{OC} value is a result of each given light intensity.

dependent on the electrolyte,[49] is higher in the cobalt-based DSCs than in the I$_3^-$/I$^-$-containing DSCs (Table 7). As the voltage of the cell is higher and R_t becomes insignificant, the more positive redox potential of the cobalt mediators and simpler charge transfer kinetics result in a higher C_μ. The relatively high R_{rec} of the I$_3^-$/I$^-$-based DSCs results in the larger values of electron lifetime presented in Fig. 5b and Tables 6 and 7; this decreases exponentially upon increasing the light intensity. However, the high C_μ of the cobalt-based DSCs results in the larger J_{SC} seen for these DSCs (Table 3).

If one considers V_{OC}, R_{rec} and C_μ for DSCs with [Co(bpy)$_3$]$^{2+/3+}$ and [Co(phen)$_3$]$^{2+/3+}$, it appears that the [Co(phen)$_3$]$^{2+/3+}$ electrolyte should be superior of the two in terms of DSC efficiency. However, its higher resistance to mass transport is detrimental, limiting the J_{SC} to a greater extent, and resulting in the [Co(bpy)$_3$]$^{2+/3+}$ electrolyte having the highest DSC efficiency. On the other hand, in the iodide systems, R_d is insignificant, but here, the much lower V_{OC} and, despite the high R_{rec}, the moderate chemical capacitance result in the more modest overall DSC performance.

Conclusions

The performances of DSCs containing the sensitizers [Cu(**1**)(**2**)]$^+$, [Cu(**1**)(**3**)]$^+$ and [Cu(**1**)(**4**)]$^+$ combined with each of the redox shuttles [Co(bpy)$_3$]$^{3+/2+}$ [Co(phen)$_3$]$^{3+/2+}$ or I$_3^-$/I$^-$ have been investigated. For all three dyes, the photoconversion efficiency is enhanced by using [Co(bpy)$_3$]$^{2+/3+}$ or [Co(phen)$_3$]$^{2+/3+}$ in place of I$_3^-$/I$^-$. This is consistent with the faster charge-transfer kinetics and more positive redox potential of [Co(bpy)$_3$]$^{2+/3+}$ or [Co(phen)$_3$]$^{2+/3+}$ *versus* I$_3^-$/I$^-$. The best performing DSC contains the [Cu(**1**)(**4**)]$^+$ dye combined with a [Co(bpy)$_3$]$^{2+/3+}$ redox mediator; value of $\eta = 3.47$ and 3.69% for duplicate DSCs relative to $\eta = 7.12\%$ for an N719 reference DSC are the highest efficiencies achieved for a heteroleptic copper(ı) sensitizer using our 'surfaces-as-ligands' approach. The results of an EIS study demonstrate that the improved performance of the [Co(bpy)$_3$]$^{2+/3+}$ or [Co(phen)$_3$]$^{2+/3+}$-containing DSCs compared to the devices containing the I$_3^-$/I$^-$ electrolyte is mainly due to the more rapid charge exchange kinetics exhibited by the cobalt redox mediators and their more positive redox potentials. This results in an improved chemical capacitance and V_{OC}. However, on going from I$_3^-$/I$^-$ to cobalt-based cells, the recombination rate increases as a consequence of the faster kinetics. In the present investigation which uses 3-methoxypropionitrile as solvent, [Cu(**1**)(**4**)]$^+$ combined with the [Co(bpy)$_3$]$^{2+/3+}$ electrolyte leads to the highest DSC efficiency. However, given the EIS parameters and the high V_{OC} for the [Co(phen)$_3$]$^{2+/3+}$ system, it seems likely that a solvent with a lower viscosity should render the [Co(phen)$_3$]$^{2+/3+}$ electrolyte the more advantageous, and we are currently investigating this option.

Acknowledgements

13002 | *J. Mater. Chem. A*, 2016, **4**, 12995–13004

This journal is © The Royal Society of Chemistry 2016

Notes and references

1 M. Grätzel, *Acc. Chem. Res.*, 2009, **42**, 1788; M. Grätzel, *Inorg. Chem.*, 2005, **44**, 6841; M. Grätzel, *J. Photochem. Photobiol., C*, 2003, **4**, 145 and references therein.

2 *Dye Sensitized Solar Cells*, ed. K. Kalyanasundaram, CRC Press, Boca Raton, 2010.

3 A. Mishra, M. Fischer and P. Bäuerle, *Angew. Chem., Int. Ed.*, 2009, **48**, 2474.

4 A. Yella, H.-W. Lee, H. N. Tsao, C. Yi, A. K. Chandiran, M. K. Nazeeruddin, E. W.-G. Diau, C.-Y. Yeh, S. M. Zakeeruddin and M. Grätzel, *Science*, 2011, **334**, 629.

5 T. Higashino and H. Imahori, *Dalton Trans.*, 2015, **44**, 448.

6 A. Hagfeldt, G. Boschloo, L. Sun, L. Kloo and H. Pettersson, *Chem. Rev.*, 2010, **110**, 6595.

7 A. Hagfeldt and M. Grätzel, *Acc. Chem. Res.*, 2000, **33**, 269.

8 Y. Xie, Y. Tang, W. Wu, Y. Wang, J. Liu, X. Li, H. Tian and W.-H. Zhu, *J. Am. Chem. Soc.*, 2015, **137**, 14055.

9 H. Ozawa, Y. Okuyama and H. Arakawa, *ChemPhysChem*, 2014, **15**, 1201.

10 K. Kakiage, Y. Aoyama, T. Yano, T. Otsuka, T. Kyomen, M. Unno and M. Hanaya, *Chem. Commun.*, 2014, **50**, 6379.

11 C.-Y. Chen, M. Wang, J.-Y. Li, N. Pootrakulchote, L. Alibabaei, C.-H. Ngoc-le, J.-D. Decoppet, J.-H. Tsai, C. Grätzel, C.-G. Wu, S. M. Zakeeruddin and M. Grätzel, *ACS Nano*, 2009, **3**, 3103.

12 S. Mathew, A. Yella, P. Gao, R. Humphry-Baker, B. F. E. Curchod, N. Ashari-Astani, I. Tavernelli, U. Rothlisberger, M. K. Nazeeruddin and M. Grätzel, *Nat. Chem.*, 2014, **6**, 242.

13 K. Kakiage, Y. Aoyama, T. Yano, K. Oya, T. Kyomen and M. Hanaya, *Chem. Commun.*, 2015, **51**, 6315.

14 Z. Yao, M. Zhang, H. Wu, L. Yang, R. Li and P. Wang, *J. Am. Chem. Soc.*, 2015, **137**, 3799.

15 K. Kakiage, Y. Aoyama, T. Yano, K. Oya, J.-I. Fujisawa and M. Hanaya, *Chem. Commun.*, 2015, **51**, 15894.

16 N. Alonso-Vante, J.-F. Nierengarten and J.-P. Sauvage, *J. Chem. Soc., Dalton Trans.*, 1994, 1649.

17 N. Armaroli, G. Accorsi, F. Cardinali and A. Listorti, *Top. Curr. Chem.*, 2007, **280**, 69 and references therein.

18 A. Lavie-Cambot, M. Cantuel, Y. Leydet, G. Jonusauskas, D. M. Bassani and N. D. McClenaghan, *Coord. Chem. Rev.*, 2008, **252**, 2572.

19 S. Sakaki, T. Kuroki and T. Hamada, *J. Chem. Soc., Dalton Trans.*, 2002, 840.

20 T. Bessho, E. C. Constable, M. Graetzel, A. Hernandez Redondo, C. E. Housecroft, W. Kylberg, M. K. Nazeeruddin, M. Neuburger and S. Schaffner, *Chem. Commun.*, 2008, 3717.

21 C. E. Housecroft and E. C. Constable, *Chem. Soc. Rev.*, 2015, **44**, 8386 and references therein.

22 M. Magni, P. Biagini, A. Colombo, C. Dragonetti, D. Roberto and A. Valore, *Coord. Chem. Rev.*, 2016, **322**, 69.

23 H. J. Snaith, *Energy Environ. Sci.*, 2012, **5**, 6513.

24 H. J. Snaith, *Nat. Photonics*, 2012, **6**, 337.

25 F. J. Malzner, S. Y. Brauchli, E. C. Constable, C. E. Housecroft and M. Neuburger, *RSC Adv.*, 2014, **4**, 48712.

26 M. Sandroni, L. Favereau, A. Planchat, H. Akdas-Kilig, N. Szuwarski, Y. Pellegrin, E. Blart, H. Le Bozec, M. Boujtita and F. Odobel, *J. Mater. Chem. A*, 2014, **2**, 9944.

27 Z. Yu, M. Gorlov, J. Nissfolk, G. Boschloo and L. Kloo, *J. Phys. Chem. C*, 2010, **114**, 10612.

28 G. Boschloo and A. Hagfeldt, *Acc. Chem. Res.*, 2009, **42**, 1819.

29 Z. Sun, M. Liang and J. Chen, *Acc. Chem. Res.*, 2015, **48**, 1541.

30 B. Pashaei, H. Shahroosvand and P. Abbasi, *RSC Adv.*, 2015, **5**, 94814.

31 S. M. Feldt, E. A. Gibson, E. Gabrielsson, L. Sun, G. Boschloo and A. Hagfeldt, *J. Am. Chem. Soc.*, 2010, **132**, 16714.

32 T. W. Hamann, *Dalton Trans.*, 2012, **41**, 3111.

33 See for example: S. Nakade, Y. Makimoto, W. Kubo, T. Kitamura, Y. Wada and S. Yanagida, *J. Phys. Chem. B*, 2005, **109**, 3488; S. Yun, Y. Liu, T. Zhang and S. Ahmad, *Nanoscale*, 2015, 7, 11877.

34 H. Nusbaumer, S. M. Zakeeruddin, J.-E. Moser and M. Grätzel, *Chem.–Eur. J.*, 2003, **9**, 3756.

35 B. Bozic-Weber, E. C. Constable, S. O. Fürer, C. E. Housecroft, L. J. Troxler and J. A. Zampese, *Chem. Commun.*, 2013, **49**, 7222.

36 L. N. Ashbrook and C. M. Elliott, *J. Phys. Chem. C*, 2013, **117**, 3853.

37 B. Bozic-Weber, S. Y. Brauchli, E. C. Constable, S. O. Fürer, C. E. Housecroft, F. J. Malzner, I. A. Wright and J. A. Zampese, *Dalton Trans.*, 2013, **42**, 12293.

38 S. O. Fürer, B. Bozic-Weber, M. Neuburger, E. C. Constable and C. E. Housecroft, *RSC Adv.*, 2015, **5**, 69430.

39 See for example: B. M. Klahr and T. W. Hamann, *J. Phys. Chem. C*, 2009, **113**, 14040.

40 See for example: S. Carli, E. Busatto, S. Caramori, R. Boaretto, R. Argazzi, C. J. Tipson and C. A. Bignozzi, *J. Phys. Chem. C*, 2013, **117**, 5142.

41 B. Bozic-Weber, E. C. Constable, C. E. Housecroft, P. Kopecky, M. Neuburger and J. A. Zampese, *Dalton Trans.*, 2011, **40**, 12584.

42 H. Zabri, I. Gillaizeau, C. A. Bignozzi, S. Caramori, M.-F. Charlot, J. Cano-Boquera and F. Odobel, *Inorg. Chem.*, 2003, **42**, 665 and references cited therein.

43 See for example: M. Nilsing, P. Persson and L. Ojamäe, *Chem. Phys. Lett.*, 2005, **415**, 375.

44 Y. Ooyama and Y. Harima, *Eur. J. Org. Chem.*, 2009, 2903.

45 F. J. Malzner, S. Y. Brauchli, E. Schönhofer, E. C. Constable and C. E. Housecroft, *Polyhedron*, 2014, **82**, 116.

46 A. Fischer, H. Pettersson, A. Hagfeldt, G. Boschloo, L. Kloo and M. Gorlov, *Sol. Energy Mater. Sol. Cells*, 2007, **91**, 1062.

47 J. Wu, Z. Lan, J. Lin, M. Huang, Y. Huang, L. Fan and G. Luo, *Chem. Rev.*, 2015, **115**, 2136.

48 S. M. Feldt, G. Wang, G. Boschloo and A. Hagfeldt, *J. Phys. Chem. C*, 2011, **115**, 21500.

This journal is © The Royal Society of Chemistry 2016

J. Mater. Chem. A, 2016, **4**, 12995–13004 | **13003**

49 F. Fabregat-Santiago, J. Bisquert, G. Garcia-Belmonte, G. Boschloo and A. Hagfeldt, *Sol. Energy Mater. Sol. Cells*, 2005, **87**, 117.

50 J. Bisquert, F. Fabregat-Santiago, I. Mora-Sero, G. Garcia-Belmonte and S. Gimenez, *J. Phys. Chem. C*, 2009, **113**, 17278.

51 H. Nusbaumer, J.-E. Moser, S. M. Zakeeruddin, M. K. Nazeeruddin and M. Graetzel, *J. Phys. Chem. B*, 2001, **105**, 10461.

52 A. Colombo, C. Dragonetti, M. Magni, D. Roberto, F. Demartin, S. Caramori and C. A. Bignozzi, *ACS Appl. Mater. Interfaces*, 2014, **6**, 13945.